

PHOTOCATALYTIC ACTIVITY OF MESOPOROUS TITANIUM DIOXIDE STABILIZED WITH LANTHANUM IN THE GAS-PHASE OXIDATION OF ETHANOL

N. I. Ermokhina,¹ V. V. Shvalagin,¹ N. I. Romanovska,¹ N. A. Sydorova,¹
P. A. Manoryk,¹ R. Yu. Barakov,¹ M. M. Shcherbatyuk,²
D. O. Klymchuk,² and A. M. Puziy³

UDC 541.145

Samples of mesoporous anatase (TiO₂) with crystallites of not more than 10 nm in size stabilized with lanthanum(III) ions, which are 3-4 times more photochemically active than the commercial TiO₂ product Evonik P25 in the total gas-phase oxidation of ethanol, were obtained by the sol-gel method. It was established that hydrothermal treatment and addition of lanthanum increase the photocatalytic activity. This may be due to decrease in the size of the crystallites that form its secondary mesoporous structure and also to increase in the size of the pores, which favors adsorption of the substrate molecules and desorption of the reaction products into the gas phase.

Key words: mesoporous TiO₂, anatase, lanthanum, gas-phase oxidation of ethanol.

Titanium dioxide nanomaterials with controllable morphology and texture are in great demand in various branches of industry, biology, and medicine. Titanium dioxide, an adsorbent and a semiconductor with a broad band gap of 3.2 eV, is one of the most promising photocatalysts for the degradation of toxic metal ions, the decomposition of water (with the formation of hydrogen and oxygen), and the oxidation of harmful organic compounds to simple inorganic molecules of carbon dioxide and water, and this can make a significant contribution to solution of the energy and ecological problems of modern society [1, 2].

The activity of the photocatalyst is determined by a combination of various parameters: degree of crystallinity, phase composition, size of crystallites, developed surface area, surface organization, porosity, etc. [1, 2]. For this reason mesoporous nanocrystalline TiO₂ (meso-nc-TiO₂) is of special interest among the nanomaterials in that it has the necessary set of parameters. As far back as 1995 the authors of [3] put forward their own modified version of the sol-gel method and synthesized for the first time mesoporous TiO₂ with a large surface area, thereby demonstrating good prospects for the

¹ L. V. Pysarzhevsky Institute of Physical Chemistry, National Academy of Sciences of Ukraine, Prospekt Nauky, 31, Kyiv 03028, Ukraine. E-mail: vitaliy.shvalagin@gmail.com.

²M. G. Kholodnyi Institute of Botany, National Academy of Sciences of Ukraine, Vul. Tereshchenkivs'ka, 2, Kyiv 01601, Ukraine.

³Institute for Sorption and Problems of Endoecology, National Academy of Sciences of Ukraine, Vul. Henerala Naumova, 13, Kyiv 03164, Ukraine.

TABLE 1. The Textural Characteristics of meso-nc-TiO₂ Samples and Their Photocatalytic Characteristics in the Gas-Phase Oxidation of Ethanol

Sample	Additives		S_{sp} , m ² /g	V_{por} , cm ³ /g	D_{por} , nm	Size of crystallites, nm	Total photodecomposition time, min	
	DDMEABr	La ³⁺					Ethanol	Acetaldehyde
T1	–	+	71	0.13	7.0	6.6	100	180
T1H	–	+	128	0.54	18.6	6.3	60	80
T2	+	+	71	0.14	7.0	6.8	85	125
T2H	+	+	131	0.59	15.9	6.6	80	115
T3	+	+	69	0.20	13.9	9.9	140	215
T3H	+	+	137	0.97	17.3	7.2	80	120
T4	+	–	33	0.06	5.3	9.9	>350	>350
T4H	+	–	95	0.46	19.4	8.3	90	140
Evonik P25	–	–	50	–	–	25	140	340

development of approaches to the synthesis of mesoporous TiO₂. By varying the conditions of the process with the use of templates and by introducing various additives that affect the interaction between the TiO₂ particles at a specific stage in the formation of the porous framework it is possible to obtain unique nanomaterials with a given morphology and a texture with a large specific surface area [4]. It should be noted that today the sol–gel method remains one of the best methods for the production of mesoporous metal oxides.

The production of an effective meso-nc-TiO₂ photocatalyst always involves the solution of problems in the complete removal of the template and crystallization of the TiO₂ samples during heat treatment (at ~500 °C) in order to achieve their full photocatalytic potential and to prevent total destruction of the mesopores as a result of extensive growth of the crystallites [5]. Since the most photoactive crystalline modification of TiO₂ is anatase, most approaches have been directed toward the production of mesoporous nanodimensional TiO₂ with anatase walls. By including La³⁺ ions, which inhibit the anatase → rutile transformation, in the reaction mixture it is possible to increase the thermal stability, textural characteristics, and photocatalytic activity of mesoporous TiO₂ materials significantly [6-11]. The authors explain the role of these cations in stabilization of the structure of the mesoporous TiO₂ by insertion of the rare-earth cation into the framework of the oxide system. When the lanthanum dopant, which is more electropositive than titanium, forms an La–O bond partial transfer of electrons from the La–O bond to the Ti–O bond occurs, leading to strengthening of the Ti–O bond. We have also demonstrated that small amounts of lanthanum ions have a stabilizing effect [12].

Earlier we proposed approaches to the sol–gel production of thermally stable mesoporous nanocrystalline TiO₂ (meso-nc-TiO₂) (anatase crystallites in the order of 10 nm) using titanium tetrabutoxide (TBOT) and dibenzo-18-crown-6 (DB18C6) as template in the presence of small additions of La³⁺ ions or of La³⁺ ions in conjunction with the cationic surfactant dodecyldimethylethylammonium bromide (DDMEABr) by hydrothermal treatment (HTT) followed by the necessary calcination at 500 °C [12-14]. The presence of the additives has a significant effect on the degree of crystallization, morphology, and texture of the TiO₂ samples. It was established that the samples of meso-nc-TiO₂ obtained in the presence of palmitic acid as surfactant additive have significantly higher photocatalytic activity in the release of hydrogen from water–ethanol mixtures and gas-phase oxidation of ethanol and benzene by atmospheric oxygen [15].

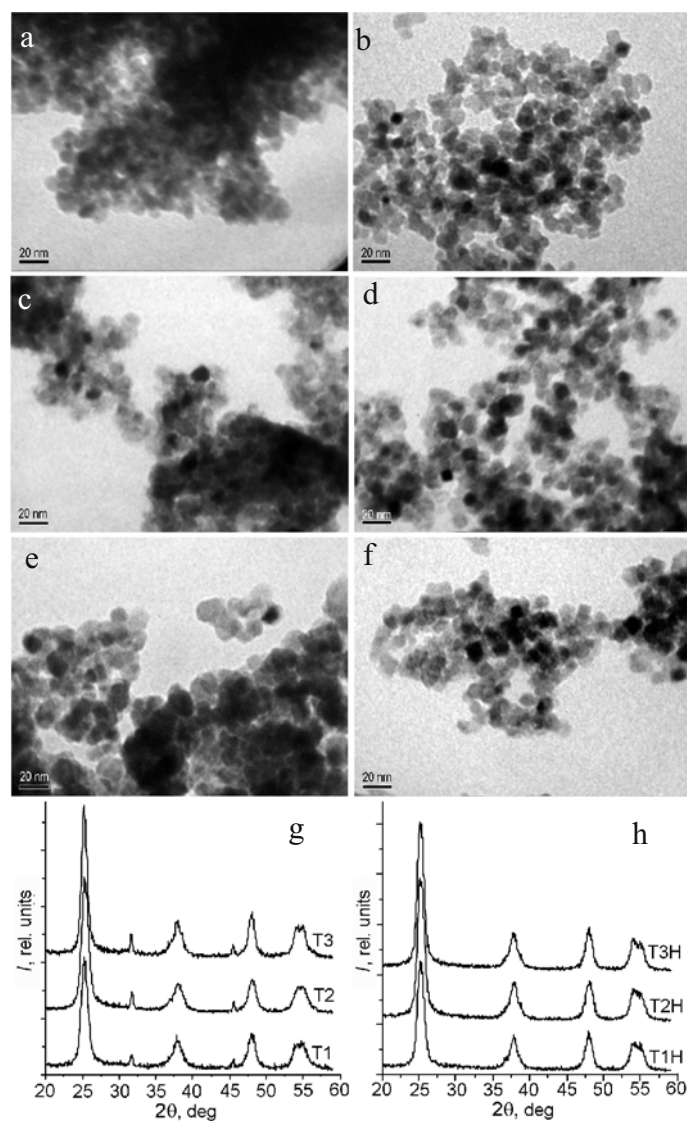


Fig. 1. TEM images of samples of meso-nc-TiO₂ T1 (a), T1H (b), T2 (c), T2H (d), T3 (e), and T3H (f) and their diffractograms (g, h).

In the present work the photocatalytic properties of samples of meso-nc-TiO₂, obtained by the methods mentioned above with the addition of small amounts of La³⁺ ions or of La³⁺ ions in conjunction with DDMEABr, were investigated in the gas-phase oxidation of ethanol by atmospheric oxygen.

Titanium(IV) tetrabutoxide, dodecyldimethylethylammonium bromide, dibenzo-18-crown-6 (Fluka), LaCl₃·7H₂O, *n*-butanol, NaCl (Khimlaborreaktiv), ethanol, and Evonik P25 TiO₂ were used.

The samples of meso-nc-TiO₂ were obtained according to our previously described modified sol-gel method [14]. The necessary amounts of the previously prepared complex of sodium with dibenzo-18-crown-6 [Na(DB18C6)]Cl, the salt LaCl₃·7H₂O, and the surfactant DDMEABr were dissolved successively by heating in butanol (~50 °C). The sodium complex was used because of the low solubility of the crown ether in butanol. After cooling to room temperature a solution of titanium tetrabutoxide in butanol (1 : 2) was added dropwise over 3 h with vigorous stirring. Hydrolysis was realized in moist air, for which the reaction mixture was left (without stirring) under a glass cover in a moist atmosphere at room temperature until the layer of white precipitate had stopped increasing. Approximately half of the precipitate was separated from the mother solution

by decantation, placed in a Petri dish, and dried at 90 °C for 1 h. It was then calcined at 500 °C for 4 h. The remaining deposit was subjected to hydrothermal treatment at 175 °C for 24 h. The deposit was separated from the mother solution and dried in a Petri dish in air at 90 °C for 1 h and calcined in air at 500 °C for 4 h. All the samples were white powders. The samples of meso-nc-TiO₂ prepared under various conditions were designated as T_n and T_nH, where *n* is the number of the sample and H represents hydrothermal treatment. The molar composition of the reaction mixture used for synthesis of the samples was as follows: *n* = 1, 0.01La³⁺ : 1.0TBOT : 0.12[Na(DB18C6)]Cl : 78.0BuOH; *n* = 2, 0.01La³⁺ : 1.0TBOT : 0.12[Na(DB18C6)]Cl : 0.02DDMEABr : 78.0BuOH; *n* = 3, 0.01La³⁺ : 1.0TBOT : 0.12[Na(DB18C6)]Cl : 0.02DDMEABr : 39.0BuOH; *n* = 4, 1.0TBOT : 0.12[Na(DB18C6)]Cl : 0.02DDMEABr : 78.0BuOH.

A DRON-3M diffractometer (CuK_α) was used for X-ray diffraction analyzes of the crystal structure of the samples. The average size of the TiO₂ crystallites was calculated from the width of the diffraction peak of anatase (101) for 2θ = 25.4° using the familiar Scherrer equation.

Transmission (TEM) and scanning (SEM) electron photomicrographs were obtained on JEOL JEM 1230 and JSM-6060LA microscopes.

The adsorption/desorption isotherms of N₂ were recorded at -196 °C on the Quantachrome Autosorb-6 system. Before adsorption the sample was evacuated at 200 °C for 20 h. The specific surface area (*S*_{sp}) and the average pore diameter (*D*_{por}) were determined by the BET and BJH methods respectively.

The size distribution of the pores was calculated from the desorption branch of the isotherm by the NLDFT method and a cylindrical model of the pores. The total amount of N₂ adsorbed at *p/p*₀ = 0.997 was used to determine the total volume of pores (*V*_{por}).

The photocatalytic activity of the obtained samples of meso-nc-TiO₂ was investigated in the model gas-phase oxidation of ethanol in a 150-cm³ glass reactor fitted with a membrane for inserting the substrate and sampling. We added 3.4·10⁻⁵ mol of ethanol to the reactor in the liquid form by means of a microsyringe. Titanium dioxide (50 mg) was pressed onto a 1×3 cm subshute and placed in the reactor. After delivery of the sample the gaseous mixture in the reactor was agitated with a magnetic stirrer without irradiation until the alcohol had completely evaporated (~2 h) and adsorption equilibrium had been established. The samples were then exposed to focused light (λ = 310-390 nm) with a DRSh-1000 mercury lamp fitted with special light filters. In order to prevent heating of the gas mixture in the system by the light flux a cuvette with a thickness of 2 cm filled with twice-distilled water was placed between the light filter and the reactor. The intensity of the incident light was 5·10⁻⁶ mol quanta·min⁻¹. The concentrations of the initial ethanol and of the intermediate product acetaldehyde were determined by chromatography. The industrial TiO₂ catalyst Evonik P25 was used as reference.

The physical characteristics of the meso-nc-TiO₂ samples obtained in the presence of small additions of La³⁺ ions and of La³⁺ ions in conjunction with the surfactant are presented in Table 1. As seen, the textural characteristics of the T4 and T4H samples obtained in the absence of La³⁺ ions used for comparison are lower than the corresponding values for the T2 and T2H samples. Increase in the concentration of the initial reagents (the T2, T2H and T3, T3H samples) leads to increase in the volume of the pores, and in the case without hydrothermal treatment (the T2 and T3 samples) it is accompanied also by a twofold increase in the diameter of the pores. As follows from comparison of the textural characteristics of the samples in Table 1, hydrothermal treatment of the sample before calcination leads to radical changes both in the specific surface area and in the volume and diameter of the pores. For instance, the respective characteristics of the calcined T3 sample and of the T3H sample with previous hydrothermal treatment are as follows: specific surface area 69 and 137 m²·g⁻¹; volume of pores 0.21 and 0.98 cm³·g⁻¹; diameter of pores 12.5 and 17.5 nm.

According to the data from TEM (Fig. 1a-f) all the heat-treated samples of TiO₂ exhibit uniformity and spherical form in primary particles with sizes of about 10 nm. At the same time, a steady relationship is observed: the crystallites of the hydrothermally treated samples are always smaller than the crystallites of the corresponding samples that had not been subjected to hydrothermal treatment. The T3 and T3H samples, which have crystallites with sizes of 9.9 and 7.2 nm respectively, can be cited as examples (Fig. 1e, f). The sizes of the anatase crystallites calculated from the integrated width of the diffraction peak (2θ = 25.4°) using the Scherrer equation lie in the range of 6.6-9.9 nm (Table 1).

Figure 1g, h shows the diffractograms of the samples of meso-nc-TiO₂ produced under various conditions. All the peaks were identified as reflections of the crystalline phase of anatase with the complete absence of any signs of brookite and rutile crystalline phases. In addition to the broad peaks of anatase the diffractograms of the samples obtained without

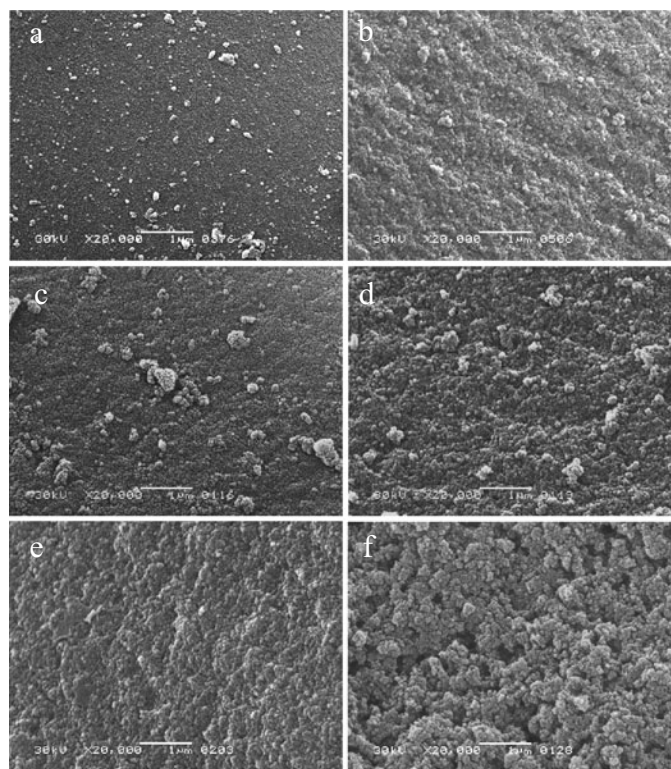
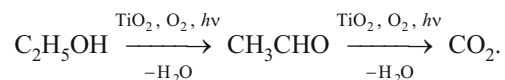


Fig. 2. SEM images of samples of meso-nc-TiO₂: a) T1; b) T1H; c) T2; d) T2H; e) T3; f) T3H.

hydrothermal treatment (Fig. 1g) contain three peaks the appearance of which must clearly be attributed to the presence of NaCl. Thus, a similar pattern was observed in [16], where a very weak broad peak at 27.8° (2θ) and two narrow peaks at 32° and 45.5° (2θ) belong to NaCl occluded by the main product during synthesis. Calcination of the intermediate products (gels) does not lead to removing the NaCl impurity from the TiO₂ samples (the T1, T2, and T3 samples), but pure samples of meso-nc-TiO₂ (T1H, T2H, T3H) may be obtained by a combination of hydrothermal treatment and subsequent calcination, as is confirmed by their diffractograms (Fig. 1h). The main diffraction peaks are indexed as (101), (004), (200), (105), and (211) reflections of the anatase phase (JCPDS 21-1272).

Figure 2a-f shows SEM images of the meso-nc-TiO₂ samples, which make it possible to reach conclusions about their morphology. In [13, 14] it was shown that mesoporous hierarchical TiO₂ microspheres with sizes in the order of 1-3 μm are formed in this system in the absence of La³⁺ ions (including the T4 and T4H samples). The microspheres are formed by spherical secondary nanoparticles of between 30 and 55 nm in size, which in turn consist of primary spherical particles (crystallites of anatase) of about 10 nm. As seen from Fig. 2a-f, in the presence of La³⁺ ions particles of micrometer size are not formed at all in all cases, i.e., the addition of a small amount of lanthanum leads to revolutionary changes in the morphology of the samples. The samples represent porous uniform materials that consist of particles of spherical (or spheroidal) form not exceeding 50 nm in size. These nanoparticles (secondary) are formed by aggregation of the anatase crystallites (the primary particles) measuring 6.6-9.9 nm (Fig. 1a-f). The mesopores in all the samples represent a porous space that is formed by the secondary nanoparticles during agglomeration.

The photocatalytic activity of the meso-nc-TiO₂ samples in the gas-phase oxidation of ethanol was investigated:



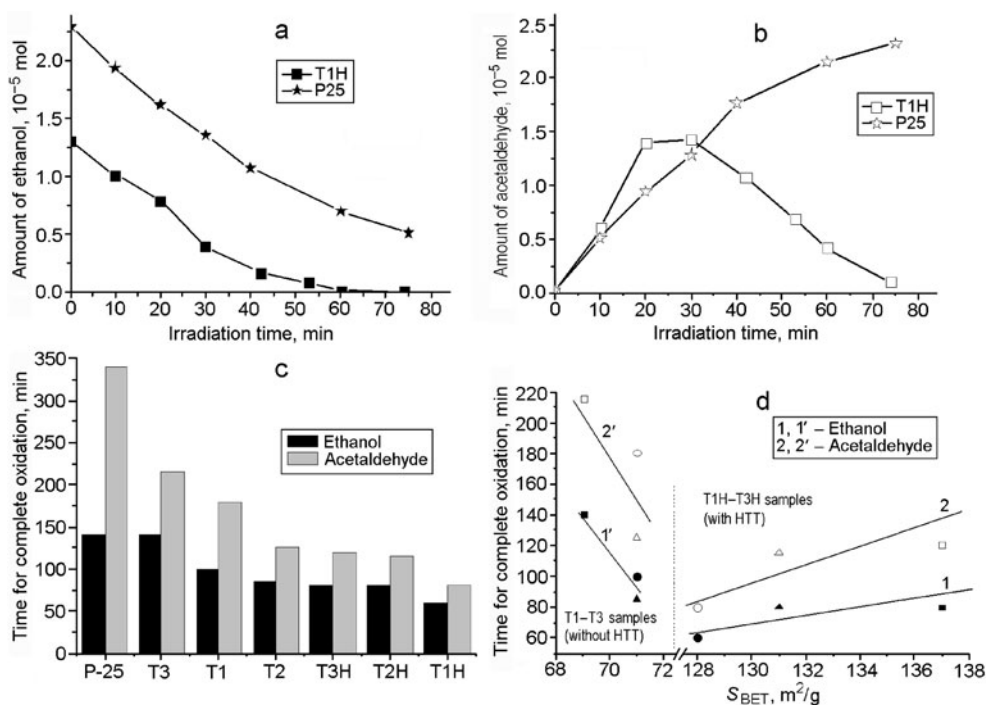


Fig. 3. Kinetic curves for oxidation of ethanol (a) and also for accumulation and oxidation of the intermediate product acetaldehyde (b) with samples T1H and Evonik P25, the time for complete oxidation of ethanol and acetaldehyde in the system with studied samples (c) and the dependence of the time for complete oxidation of ethanol and acetaldehyde on the specific surface area of T1-T3 samples obtained without HTT (1' and 2': ●, ○ T1; ▲, △ T2; ■, □ T3), and T1H-T3H samples obtained with HTT (1 and 2: ●, ○ T1H; ▲, △ T2H; ■, □ T3H) (d).

This reaction is used as a model for determination of the activity of a photocatalyst in the oxidation of organic substrates [17, 18]. In the oxidation of ethanol to CO_2 the variation of the concentration of both ethanol (the initial substrate) and acetaldehyde (the intermediate product) in the reaction mixture was monitored. The accumulation of the toxic intermediate product in the gas phase can often become a serious problem preventing use of such process for the purification of air from organic impurities.

The kinetic curves for variation of the ethanol and acetaldehyde content for the T1H and Evonik P25 samples are presented in Fig. 3a, b as an example. As seen, decrease of the ethanol content in the system is accompanied by the formation, accumulation, and disappearance of acetaldehyde.

The time for complete oxidation of ethanol in the presence of the meso-nc- TiO_2 samples is presented in Table 1 and in Fig. 3c, which gives the following order of photoactivity:

$$T1H > T2H > T3H > T2 > T1 > T3 > \text{Evonik P25.}$$

All the meso-nc- TiO_2 samples surpass Evonik P25 significantly in photoactivity in the gas-phase oxidation of ethanol. The first sample in the presented series T1H is more than four times as photoactive as Evonik P25. The samples that have undergone HTT and have larger pore diameter and smaller crystallite size than the untreated samples exhibit higher activity than the corresponding samples that have not been subjected to hydrothermal treatment.

As follows from Table 1 and from Fig. 3d, the specific surface area and other textural characteristics are clearly not dominant factors that determine the photoactivity of the meso-nc- TiO_2 samples in the process. Thus, the T1, T2, and T3 samples (without HTT) have identical specific surface areas, but their photocatalytic activity differs significantly, while the T3 sample, which has the most developed texture among them, has the lowest photoactivity. A similar pattern is observed in the

case of the T1H, T2H, and T3H samples (with HTT); the T3H sample with the best textural characteristics has the lowest photoactivity. As seen from Table 1 and Fig. 3c, the samples that have been subjected to HTT are as a whole the most photoactive in the complete oxidation of ethanol.

As seen from Table 1, the T4 and T4H samples produced without the addition of lanthanum are noticeably inferior in photoactivity to the corresponding samples T2 and T2H produced in the presence of the surfactant (DDMEABr) and lanthanum; the T2H sample is inferior in activity to the T1H sample (produced in the presence of only lanthanum as additive). At the same time, the corresponding sample T2 produced without HTT has almost the same photoactivity as T2H. Consequently, by using DDMEABr and lanthanum simultaneously as additives during the synthesis of meso-nc-TiO₂ it is possible to increase the photoactivity of the samples obtained without HTT. In the case of the T3 and T3H samples increase of the concentration of the initial reagents leads to a slight loss of photoactivity for T3H and to a marked reduction of photoactivity for T3.

It was found that in the presence of La³⁺ ions and of La³⁺ ions in conjunction with DDMEABr the samples of meso-nc-TiO₂ produced according to our previously proposed modified sol-gel method [14] exhibit high photocatalytic activity in the gas-phase oxidation of ethanol. The samples obtained with the use of HTT exhibit the highest photoactivity 3-4 times higher than the photoactivity of Evonik P25.

The key effect of HTT on the increase of the photoactivity evidently arises from the radical increase of the pore diameter in the treated samples and also from decrease in the size of the crystallites. These changes are more fundamental for the samples obtained with simultaneous addition of lanthanum and surfactant. In our opinion this effect of the pore size of the titanium dioxide on the increase of photoactivity may be due to more effective penetration of the substrate molecules into the pores of the photocatalyst and to escape of the oxidation products into the gas phase, which frees up the internal surface of the TiO₂. Here decrease in the size of the crystallites of the photocatalyst in the nanometer range will lead to the appearance of quantum-size effects and in particular to increase of the potentials of the planar TiO₂ bands and accordingly to increase in the efficiency of the photocatalytic processes involving it.

REFERENCES

1. K. Nakata and A. Fujishima, *J. Photochem. Photobiol.*, **13**, No. 3, 169-189 (2012).
2. F. Fresno, R. Portela, S. Suárez, and J. M. Coronado, *J. Mater. Chem.*, **2**, No. 9, 2863-2884 (2014).
3. D. M. Antonelli and J. Y. Ying, *Angew. Chem. Int. Ed. Engl.*, **34**, No. 18, 2014-2017 (1995).
4. X. Chen and S. S. Mao, *Chem. Rev.*, **107**, No. 7, 2891-2959 (2007).
5. A. A. Ismail and D. W. Bahnemann, *J. Mater. Chem.*, **21**, No. 32, 11686-11707 (2011).
6. S. Yuan, Q. Sheng, J. Zhang, et al., *Micropor. Mesopor. Mater.*, **110**, Nos. 2/3, 501-507 (2008).
7. C. P. Sibue, S. R. Kumar, P. Mukundan, and K. G. K. Warriar, *Chem. Mater.*, **14**, No. 7, 2876-2881 (2002).
8. W. Zhang, *Chem. Commun.*, No. 11, 1185-1186 (1998).
9. J. Liqiang, S. Xiaojun, X. Baifu, et al., *J. Solid State Chem.*, **177**, No. 10, 3375-3382 (2004).
10. D. A. H. Hanaor and C. C. Sorrell, *J. Mater. Sci.*, **46**, No. 4, 855-874 (2011).
11. M. Milanović and L. M. Nikolić, *Proc. Appl. Ceram.*, **8**, No. 4, 195-202 (2014).
12. N. I. Ermokhina, V. I. Litvin, V. G. Il'in, and P. A. Manorik, *Ukr. Khim. Zh.*, **73**, Nos. 1/2, 21-25 (2007).
13. N. I. Ermokhina, V. A. Nevinskiy, P. A. Manorik, et al., *Mater. Lett.*, **75**, 68-70 (2012).
14. N. I. Ermokhina, V. A. Nevinskiy, P. A. Manorik, et al., *J. Solid State Chem.*, **200**, 90-98 (2013).
15. A. L. Stroyuk, N. I. Ermokhina, A. V. Korzhak, et al., *Teor. Éksp. Khim.*, **51**, No. 3, 176-184 (2015). [*Theor. Exp. Chem.*, **51**, No. 3, 183-190 (2015) (English translation).]
16. G. Hu, D. Ma, M. Cheng, et al., *Chem. Commun.*, No. 17, 1948-1949 (2002).
17. O. L. Stroyuk, O. Ye. Rayevska, V. V. Shvalagin, et al., *Photochem. Photobiol. Sci.*, **12**, No. 4, 621-625 (2013).
18. C. L. Bianchi, C. Pirola, and F. Galli, *RSC Adv.*, **5**, No. 66, 53419-53425 (2015).